JOURNAL OF CATALYSIS **166,** 186–194 (1997)
ARTICLE NO. CA971534

Pt Species in Zeolite X: Catalytic Activity in ^{18}O Exchange of O_2 with Zeolitic Oxygen, $^{18}O_2$–$^{16}O_2$ Equilibration, H_2–D_2 Equilibration, and the CO–NO Reaction

J. Nováková and L. Brabec

J. Heyrovský Institute of Physical Chemistry, Academy of Sciences of the Czech Republic, Dolejškova 3, 182 23 Prague 8, Czech Republic

Received February 9, 1996; revised September 16, 1996; accepted November 11, 1996

Pt^0, Pt^{2+} and Pt_{ox} were prepared by different treatments of platinum tetrammine complexes in alkali faujasites. The observed behavior of Pt, especially in TPR experiments, provided evidence that the decomposition of ammine complexes in an oxygen stream yields predominantly Pt cations, which following reduction by hydrogen leads to the formation of small metallic clusters, whose reoxidation gives Pt_{ox} in zeolite cavities. The activity of both latter species was markedly higher than that of Pt^{2+} in the reaction studied, i.e., in the isotopic exchange of gaseous oxygen with the oxygens of the zeolite framework, in the equilibration of hydrogen and oxygen molecules ($D_2 + H_2$ and $^{18}O_2 + {}^{16}O_2$ reaction, respectively), and in the NO reduction by CO. The catalytic reactions were studied over NaX and KX zeolites. Isotopic exchange of $^{18}O_2$ with zeolitic oxygen occurred even below 400°C, oxygen activated on Pt centers (3Pt per unit cell) being spilled over to the oxygen of the zeolite skeleton. The equilibration of the gaseous oxygen molecules began above 300°C, while that of hydrogen molecules was easily measured at −78°C. © 1997 Academic Press

INTRODUCTION

In preceding papers (1, 2), the activity of Pt clusters obtained by vacuum decomposition of Pt tetrammine ions in alkali X and Y zeolites in NO reduction by CO was reported. It was found that the increasing electropositivity and size of alkali cations as well as the increasing basicity of the zeolite type enhanced the conversion.

Platinum, after the vacuum decomposition of ammonia complexes, was predominantly in the Pt^0 state (from about 80%) and formed clusters 2–4 nm in size. It was not possible to reoxidize all the Pt atoms: if the sample was oxidized after the vacuum decomposition, the amount of hydrogen needed for the following reduction was lower than would correspond to the complete oxidation of all Pt to Pt(II).

In the present paper, the behavior of more finely dispersed Pt clusters is studied. It is well known from the literature (3–9) that a slow calcination of the Pt ammine complex in zeolites followed by reduction yields highly dispersed platinum. During the calcination, two kinds of oxidized Pt species were reported: Pt^{2+} as charge balancing cation (e.g., 6, 7) and/or PtO (8). Ostgard *et al.* (10) separated these two oxidized states for Pd in zeolites using calcination of palladium tetrammine, which was claimed to give Pd^{2+}, and calcination after reduction, which most probably yielded PdO. We have employed here the same treatment for platinum and checked the behavior of calcined and after reduction recalcined samples by TPR and have followed the progress of calcination, reduction, and recalcination (and repeated reduction) by UV/VIS. Many important processes are catalyzed by supported Pt and also by Pt in zeolites, where metallic, cationic, and oxidic species can operate. The above treatments, namely calcination, reduction, and recalcination, offer a possibility to distinguish the individual Pt species (Pt^{2+}, Pt^0, and Pt_{ox}, respectively) and to examine their catalytic activity. The catalytic reactions employed were $D_2 + H_2$ equilibration (which can be related to hydrogenation), oxygen equilibration (homophase exchange) and $^{18}O_2$ exchange with zeolitic oxygen (heterophase exchange), and NO reduction by CO.

EXPERIMENTAL

Zeolites

The parent NaX (Si/Al = 1.25, supplied by Serva International, Heidelberg) and NaY (Si/Al = 2.5, supplied by VURUP, Bratislava) were ion-exchanged with $Pt(NH_3)_4Cl_2$ (Aldrich Chemicals) either for the parent sodium form at room temperature overnight (dilute solutions, complete exchange of Pt tetrammine ions) or under the same conditions for other alkali ions (Li^+, K^+, or Cs^+) which were previously exchanged for Na^+. The ion exchange of alkali ions was carried out via three times repeated treatment of NaX with 0.5 *M* solutions of the respective nitrate (for Cs, hydroxide + HNO_3) at 60°C always for 2 h (Cs, room temperature, overnight) at pH 6.4–6.7 for X zeolites, 5.4–6.2 for Y zeolites (Cs, from initial pH 5.3 to 8.2), followed by purging with deionized water until the anions were removed, dried at room temperature, and then hydrated over calcium

0021-9517/97 $25.00

TABLE 1

Characteristics of Samples Used

Sample	Composition in mol% related to 100 Al					Pt (wt%)[a]	Pt atoms per unit cell
	Pt	Li	Na	K	Cs		
PtLiX	3.5	52.9	17.0	—	—	3.2	3.0
PtLiY	4.4	41.4	31.2	—	—	2.5	2.5
PtNaX	2.9	—	89.1	—	—	2.5	2.5
PtNaY	4.4	—	88.6	—	—	2.5	2.5
PtKX	3.5	—	9.9	78.7	—	2.6	3.0
PtKY	4.6	—	2.5	85.1	—	2.5	2.6
PtCsX	2.4	—	40.8	—	36.9	1.8	2.0
PtCsY	5.2	—	28.2	—	52.2	2.6	2.9

[a] Per hydrated sample.

nitrate. The amount of Pt in hydrated samples was within 2.5–3.2 wt%. The composition of samples is given in Table 1. Prior to the measurements (for TPR see below), zeolites were evacuated for 1 h at room temperature, dehydrated at 130°C in vacuum, and calcined in an oxygen stream up to 380°C (100 ml/min, temperature increase to 130 as well as to 380°C was 2°C/min). The samples were held at 380°C for 4 h and then either used in this oxidized form (Pt^{2+}) or reduced at 350°C in a stream of hydrogen for 1 h. The recalcination and, in some cases, new reduction were also carried out. TPR measurements were performed with all the above zeolites, but catalytic reactions were examined only over PtNaX and PtKX (calcined, reduced, and recalcined). The progress of calcination, reduction, recalcination, and repeated reduction was checked by UV/VIS for PtNaX.

Gases Employed

Gases employed (99.99% purity) were supplied by Linde. Isotopically enriched O_2 (64 and 87 at.% of ^{18}O, for the equilibration reaction mixed with $^{16}O_2$) was supplied by Technabsexport (USSR (Russia)) and deuterium (99.9 at.%) by VEB Technische Gas-Werke (Germany). The latter gas was mixed with H_2 in 1 : 1 ratio.

TPR and Hydrogen Adsorption

Calcined (without previous dehydration in vacuum) or recalcined samples (100 mg) were reduced in a hydrogen/argon stream (3 vol.% of H_2, 600 ml/h, 10°C/min) and the hydrogen consumption was measured using thermal conductivity cells in the temperature range from −18 to 25°C (the temperature held until the end of hydrogen consumption) and from 25 to 400°C. Hydrogen adsorption was examined using rapid cooling from the highest temperature to room temperature.

TEM and XPS Measurements

These two techniques were employed here only for checking the dimensions of Pt clusters (TEM) and Pt/Si ratio under various treatments of Pt zeolites (XPS). Description of the experimental arrangement is given in preceding papers (1, 2).

UV/VIS

Diffuse reflectance UV/VIS spectra were recorded using a Cary 4 spectrometer equipped with a Harrick reaction chamber. The sample reflectivity was related to that of the standard using

$$R(S) = [R(S, \text{chamber})/R(S_0, \text{chamber})] \times [R(S_0)/R_{\text{standard}}],$$

where S_0 and S designate samples measured as received in the air atmosphere and after further treatment (calcination, reduction etc.). The first ratio concerns reflectivities of the sample in the Harrick chamber, while the second ratio is obtained using the common praying mantis arrangement; $R(S_0)/R(S_0, \text{chamber})$ represents apparatus correction. The Kubelka–Munk function $f(R_\infty) = (1-R_\infty)^2/2R_\infty = k/s$ (k, absorption coefficient; s, scattering coefficient) was calculated assuming that $R_\infty = R(S)$. Difference spectra were obtained by subtracting the $f(R_\infty)$ function of the sample before heating.

Weight of the sample was ~30 mg, the decomposition of the ammine complexes was carried out in an argon/oxygen stream (5 vol.% of O_2) by a temperature increase at 1°C/min to 370°C (held at this temperature for 3 h), and spectra were recorded every 10 min. After calcination, the sample was reduced in a hydrogen/argon stream (5 vol.% of H_2, 2°C/min from room temperature to 370°C) and then, after cooling, recalcined and again reduced under the same conditions as those in the preceding processes. Only the spectra at room temperature and at 370°C are shown.

^{18}O Exchange and D_2–H_2 Equilibration

The exchange of gaseous ^{18}O (64 and 87% of ^{18}O) with oxygens of the zeolite (20 mg) was measured in a static arrangement (a "batch" reactor of 400 ml) at 380°C under the pressure of 170 Pa, with mass spectrometric detection of isotopic species. For the oxygen equilibration reactions, $^{16}O_2$ and $^{18}O_2$ (87% of ^{18}O, 85 Pa of the mixture) were mixed, and the equilibration of the gas molecules was checked either at 380°C or in temperature dependence (room temperature → 380°C). The equilibration of hydrogen molecules (D_2/H_2, initially in 1 : 1 ratio) was measured at −78°C under the pressure of 200 Pa (zeolite weight, 20 mg). A Balzers QMG 420 quadrupole mass spectrometer was employed in these measurements.

CO + NO Reaction

A CO + NO mixture (200 Pa, 1 : 1) was allowed to react with 20 mg of the sample under static conditions ("batch" reactor, volume 400 cm^3). A negligible amount of the gas phase was led into the MS using a needle valve. The pressure

drop due to this inlet was negligible; when the conversion was high, the pressure decreased almost by 25% because of the reaction stoichiometry: $2CO + 2NO = N_2 + 2CO_2$. The reaction courses were compared at constant temperatures of 180, 205, and 230°C. Ion intensities 28^+, 30^+ and 44^+ (m/z) can be directly related to ($CO + N_2$), NO and CO_2 fractions, respectively. The contribution of N_2O (ion 44^+) in the gas products was negligible under these experimental conditions, as was reported earlier (1, 2), using ^{13}CO.

RESULTS

TPR of Calcined and Recalcined Samples

TPR curves of calcined and reoxidized Pt-NaX and Pt-KX zeolites are shown in Fig. 1 (left-hand side and right-hand side, respectively). It can be seen that the reduction proceeds through two to three maxima in freshly calcined samples and that, after reoxidation, the TPR maxima are shifted to lower temperatures; the high-temperature maximum disappears. This was found with all the Pt-alkali X and Pt-alkali Y zeolites employed; no special dependence of the shape or peak position of TPR curves on the presence of various alkali ions was observed.

During the TPR of reoxidized samples, adsorption and desorption of hydrogen on Pt^0 already formed occur, which follows from the negative values of hydrogen consumption (see the shadowed area on the right-hand side of Fig. 1). The amount of hydrogen consumed in the TPR of reoxidized samples is almost the same as during the TPR of freshly calcined samples, except for NaX and KX zeolites, as given in Table 2. The latter two samples exhibit a higher consumption of hydrogen after calcination; this even exceeds the amount needed for the reduction of all Pt atoms present in these zeolites, while a rough agreement between the experimental and theoretical hydrogen consumption is found for the remaining samples (Table 2).

TABLE 2

H_2 Consumed during the TPR of Calcined Samples and Samples after Recalcination, and H_2 Adsorbed on Pt^0 after the TPR during Rapid Cooling

Sample	Pt (μmol/g)[a]	TPR H_2, after calc. (μmol/g)[a]	TPR H_2, after reox. (μmol/g)[a]	Adsorption of H_2 (μmol/g)[a]	H/Pt
Pt-LiX	170	140	150	90 (100)[b]	0.6
Pt-NaX	126	220	150	66 (70)	0.5
Pt-KX	131	365	120	140 (110)	0.9
Pt-LiY	128	150	110	80 (82)	0.6
Pt-NaY	128	140	151	72 (80)	0.6
Pt-KY	127	130	160	66 (80)	0.6
Pt-CsY	133	146	150	80 (85)	0.6

[a] Per gram of hydrated sample.
[b] After reoxidation—values in brackets.

When the freshly calcined samples were treated in vacuum up to 400°C and the gases evolved were analyzed mass spectrometrically, oxygen and NO were observed above 350°C. The fraction of NO was the highest for the two above samples; in Fig. 2, the release of NO is compared for PtNaX during the Pt ammine decomposition in vacuum (Fig. 2a, a very small amount of NO at about 200°C) and during the vacuum heating of the sample, in which the ammine ions were removed by calcination (Fig. 2b). It follows that after the 4 h calcination there still remains an appreciable amount of strongly bound NO, which was observed especially for

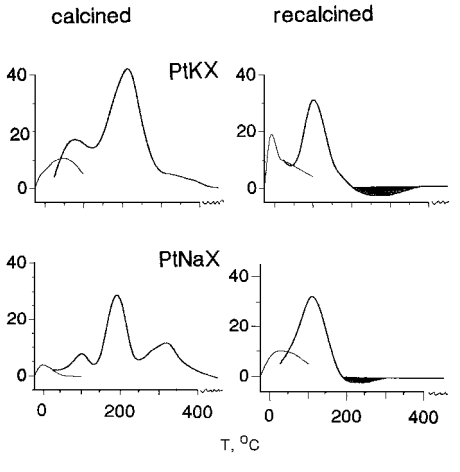

FIG. 1. TPR of calcined and recalcined PtNaX and PtKX zeolites. (Left) After calcination; (right) after reduction and recalcination. First curve: (−18°C) −RT (up to the end of reaction at RT, ca 10 min, in the figure shown as increasing temperature); second curve, RT −400°C; ∼∼∼ at the end of x axis, sample held at the final T for 20 min; shadowed area, desorption of hydrogen adsorbed at Pt reduced at lower temperatures.

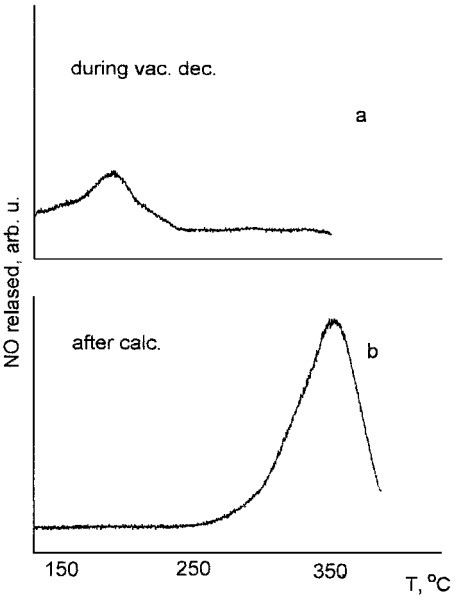

FIG. 2. NO evolved during the decomposition of Pt tetrammine ions from PtNaX during vacuum decomposition (a) and after calcination (b).

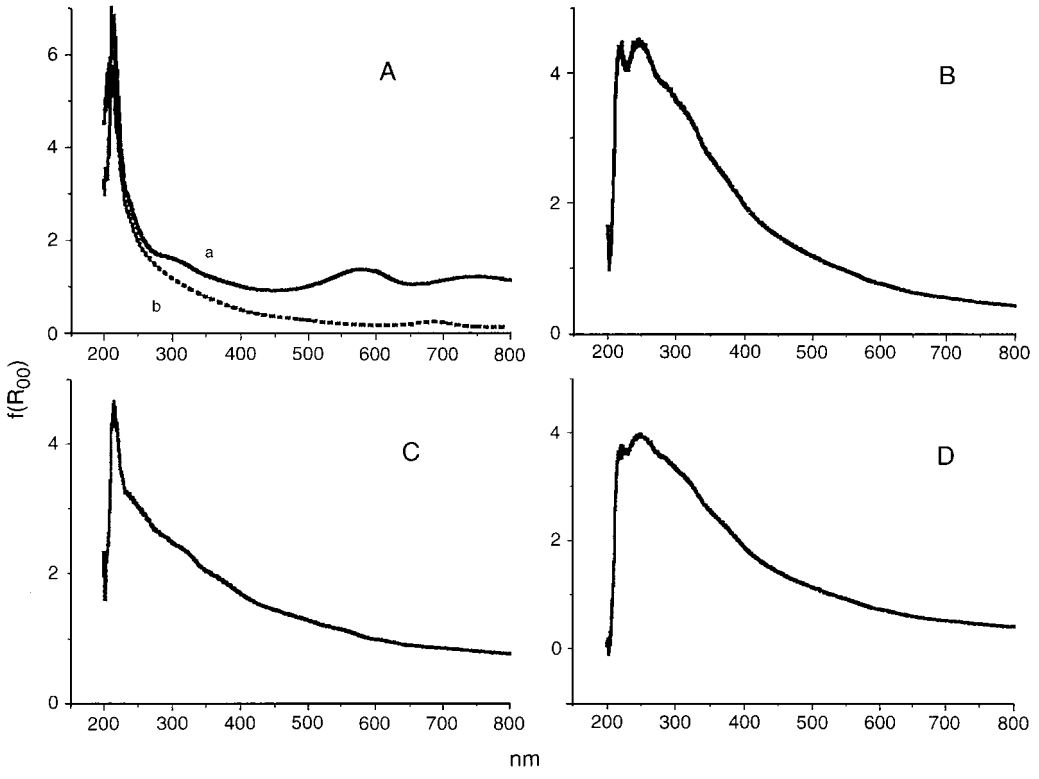

FIG. 3. UV/VIS spectra of PtNaX (A, B, C, and D). After calcination, reduction, recalcination, and repeated reduction at 370°C, respectively. (A) a, 370°C; b, room temperature (RT).

3 wt% of Pt in Na and KX zeolites after calcination (not after the recalcination).

Adsorption of Hydrogen on Pt^0 after the TPR

In Table 2, the values of hydrogen adsorbed on reduced samples during rapid cooling after the TPR measurements are also listed, together with the H/Pt ratio (hydrogen atoms adsorbed during this cooling, related to the total number of Pt atoms present in the zeolite).

UV/VIS Spectra

UV/VIS spectra recorded during the decomposition of Pt tetrammine ions in NaX via calcination and during the subsequent reduction, as well as during the Pt recalcination and repeated reduction, are shown in Figs. 3A, 3B, 3C, and 3D, respectively. It can be seen that there are differences in primary calcination and that repeated after reduction: the broad band between 550 and 630 nm is missing in recalcined samples (Fig. 3C vs Fig. 3A). This band is formed during primary calcination (in Fig. 3A shown at 370°C, curve a), but it disappears after cooling (3A, curve b). The spectra in Figs. 3B, 3C, and 3D above 500 nm are the same after cooling to room temperature.

TEM and XPS Results

TEM micrographs (measured at Bremen University, Germany) of calcined and reduced Pt in KX zeolite show rather homogeneous particle size distribution with the average cluster size of about 1–2 nm (1, 2).

XPS spectra (Pt/Si ratios compared for bulk and surface layers) do not show any difference due to various treatments of the samples.

Isotopic Exchange of Gaseous Oxygen with the Oxygen of Pt Zeolites and Equilibration of Oxygen Molecules over Pt in Zeolites

The isotopic exchange of gaseous oxygen with oxygen atoms of the zeolite, the so-called *hetero-phase exchange* (12) was examined over PtKX and PtNaX after calcination, reduction, and recalcination at 380°C (repeated reduction after recalcination yielded the same results as the primary reduction). The results are shown for the potassium form in Fig. 4A, where the beginning of the exchange (only the first 50 min) is displayed. It follows that after the first calcination the exchange is very slow and is substantially accelerated after reduction. The recalcination results in an exchange which is more similar to that with the reduced sample than with the sample after the first calcination. The same was found for PtNaX after such treatments. The initial exchange rates are given in Table 3, from which the positive effect of metallic Pt is clearly visible.

As regards the homogeneity of zeolite oxygens in the isotope exchange at 380°C, the time dependence (measured for 50 h) of ^{18}O concentration and of $\log(1-F)$ (for F see

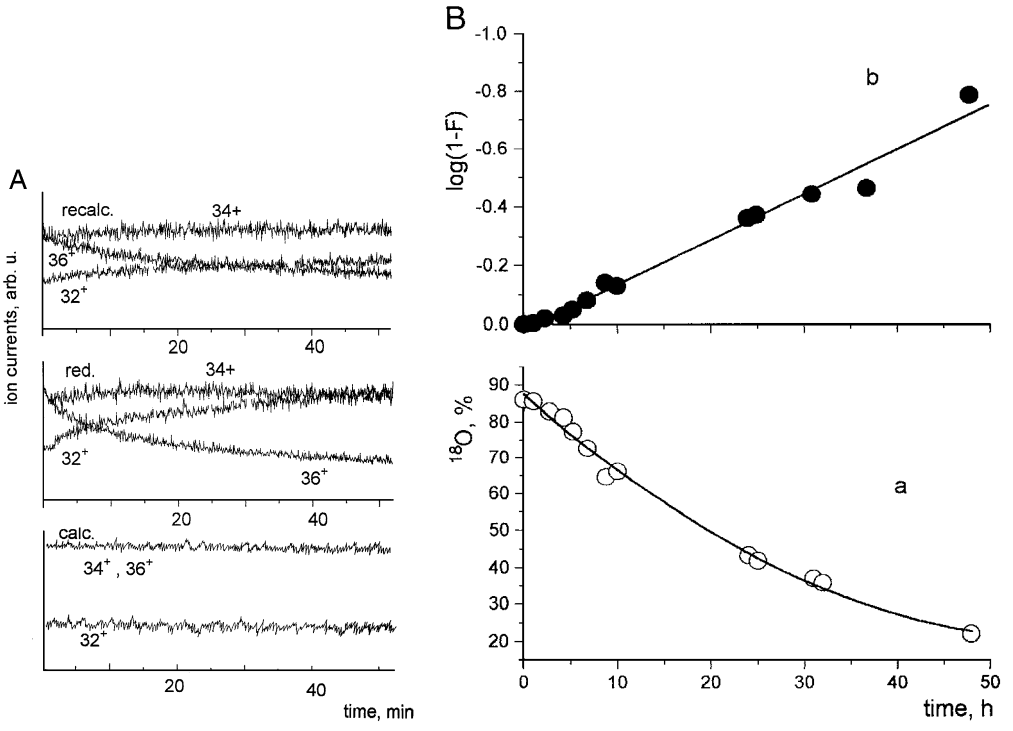

FIG. 4. ^{18}O heterophase exchange at 380°C (gaseous oxygen for zeolitic oxygens). (A) PtKX, effect of zeolite treatment, m/z 32^+, 34^+, and 36^+ for $^{16}O_2$, $^{16}O^{18}O$, and $^{18}O_2$, respectively, time dependence of molecular species at the beginning of the reaction; initial ^{18}O concentration 64%. (B) (a) PtNaX, calcined and reduced, time dependence of ^{18}O, concentration (b) $\log(1-F)$ vs time, $F=(c_0-c)/(c_0-c_\infty)$, where c_0, c and c_∞ are concentrations of ^{18}O in the gas phase at time t_0, t, and t_∞, respectively; initial ^{18}O concentration 87%.

legend of Fig. 4B) are displayed in Fig. 4B for Pt in NaX after reduction. It can be seen that the zeolite oxygens participating in the reaction are exchanged with the same rate, which follows from the straight line (reaction of the first order) in the dependence of $\log(1-F)$ vs time. The exchange was very slow over calcined samples: only about 2% of all oxygens (equal to threefold amount of Pt) was exchanged with calcined PtNaX in 24 h, in contrast to the exchange after reduction, when about 20% of all zeolite oxygens were exchanged in a similar time interval.

The Equilibration (Homophase) Exchange of Oxygen Isotopes

This reaction ($^{18}O_2 + {}^{16}O_2 \leftrightarrow 2\,{}^{16}O^{18}O$) was measured over PtKX at 380°C. The $[^{16}O^{18}O]^2/[^{16}O_2][^{18}O_2]$ ratio (in Fig. 6 denoted as Q) increased very slowly over primarily calcined PtKX and rapidly over both the reduced and the recalcined sample (Fig. 5A). To check the effect of temperature on the equilibration of oxygen molecules, the isotope mixing was examined over PtNaX starting at room temperature, as is shown in Fig. 5B. The temperature was increased from 25 to 250°C (2°C/min), the sample being then kept at this temperature for 50 min, and finally heated at the same rate to 380°C. The top curve in Fig. 5B displays the temperature course. It can be seen that the equilibration is slow below 300°C and that again, as with PtKX, the isotope mixing proceeds above 300°C with practically the same rate over reduced and recalcined samples, while it is much slower over primarily calcined PtNaX. During this equilibration, a very mild exchange with zeolite oxygens (heterophase exchange) also proceeded; however, the equilibration (homophase exchange) is clearly much more rapid than the heterophase exchange.

TABLE 3

Initial Rates of Isotopic Oxygen Heteroexchange at 380°C

Sample	Treatment	Rate × 10^{-17} (atoms/min)	Treatment	Rate × 10^{-17} (atoms/min)
PtKX	Calcination	0.88	Reduction after calcination	13.0
PtNaX	Calcination	2.5	Reduction after calcination	12.5

Note. Rates calculated from ^{18}O concentrations after 10 min reaction.

The Equilibration of Deuterium and Hydrogen

The equilibration of the 1:1 mixture proceeded very readily at −78°C except for the calcined samples, over which it was much slower. This is exemplified in Fig. 6 for Pt in NaX. The H, D equilibration over the calcined sample is shown in the bottom part of the figure and that over the reduced sample is given in the top part. Recalcination does

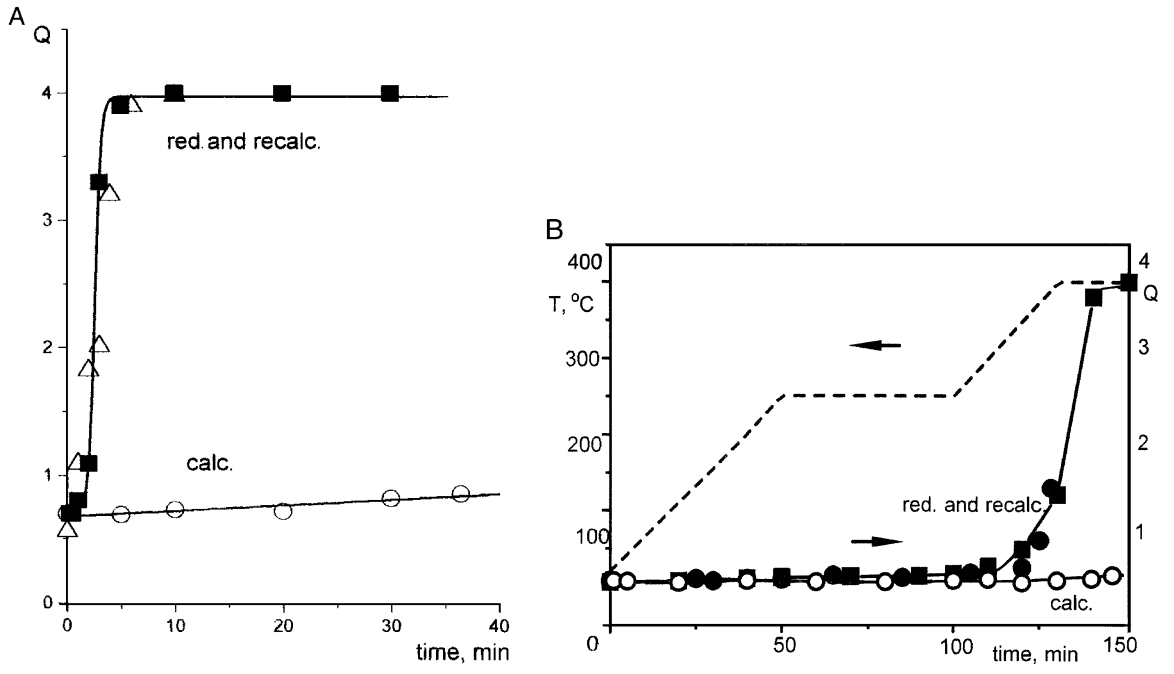

FIG. 5. Equilibration of oxygen gas molecules (homophase exchange). △ Calcination + reduction, □ recalcination, ○ calcination. (A) PtKX, 380°C, effect of zeolite treatment, (B) PtNaX, temperature dependence of equilibration, effect of zeolite treatment.

not reform the slow equilibration observed after the first calcination but gives a result very similar to that after reduction.

Isothermal NO + CO Reaction

The isothermal NO reduction by CO at 180°C is shown in Fig. 7. The reaction is compared over PtNaX after following treatments: calcination, reduction, and recalcination (from the bottom to the top curves, respectively). The conversion decreases in the sequence: red. > recalc. > calc.. This is most pronounced at the lowest temperature of 180°C (shown in the figure), is still visible at 205°C, and is almost not detectable at 230°C.

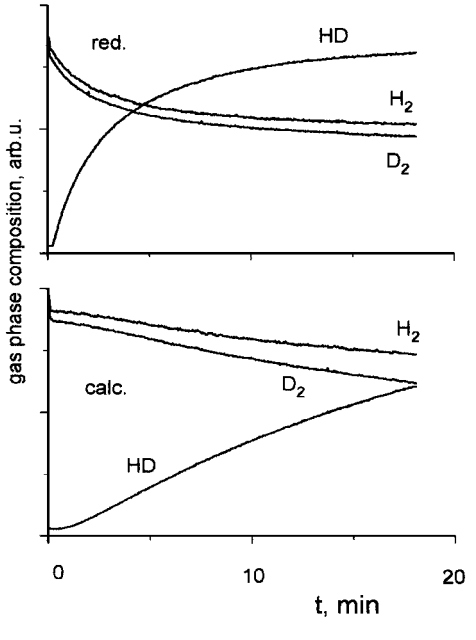

FIG. 6. $D_2 + H_2$ equilibration at −78°C PtNaX: (bottom) calcined sample; (top) reduced sample.

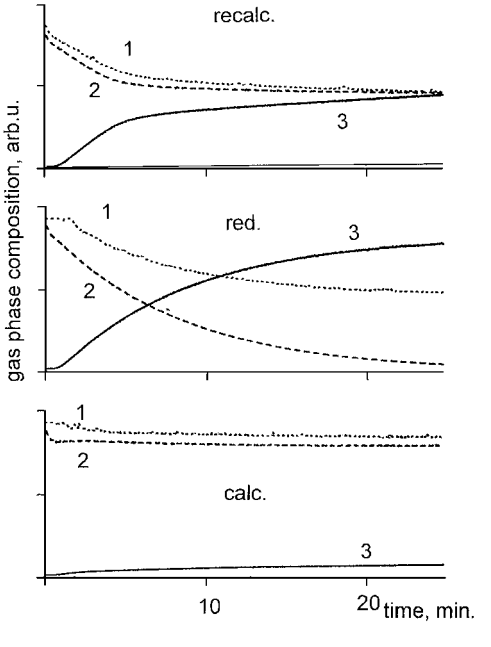

FIG. 7. Effect of PtNaX treatment on the course of CO + NO reaction at 180°C. (Bottom to top) calcined, reduced, and recalcined samples. Curve 1-($CO + N_2$); curve 2-NO, curved 3-CO_2.

DISCUSSION

TPR of Calcined and Recalcined Samples

It can be seen that all Pt^{2+} formed via calcination is reduced to Pt^0 (Table 2). The higher consumption of H_2 in PtNaX and PtKX is probably caused by reduction of NO remainders. These NO species are probably formed via oxidation of ammonia during the calcination process, as their amount is considerably higher than that formed during the vacuum decomposition of ammonia complexes and, in addition, is evolved at much higher temperature, as is shown in Fig. 2. The reduction after recalcination exhibits the consumption of hydrogen in amounts roughly corresponding to the Pt content for all samples used (Table 2) (which supports the explanation of the higher hydrogen consumption in PtNaX and PtKX rather by NO reduction than by reduction of some PtO_2 formed during the primary calcination). However, the reduction of reoxidized samples proceeds more easily, as shown by the maxima of the TPR curves being shifted to lower temperatures (Fig. 1). The amount of hydrogen adsorbed during rapid cooling after the TPR of both the calcined and recalcined samples is practically the same (Table 2, cf. values in the fifth column without and with brackets), which means that the dispersion did not change (the retention of the Pt dispersion once formed agrees with Ref. (8)). No enrichment of the superficial zeolite layers by Pt was observed (unchanged Si/Pt ratios in XP spectra). The changed character of the TPR curves after recalcination can thus be explained by assuming that predominantly Pt^{2+} cations are created after the first calcination. After reduction, Pt^0 clusters no longer compensate the charge of the skeleton and, during the recalcination, Pt_{ox} clusters are formed more probably than charge-compensating Pt^{2+}.

As regards the nature of Pt_{ox}, the amount of hydrogen consumed in reduction points to divalent Pt; the considerable decrease of the reduction temperature indicates a change in the Pt(II) character from Pt^{2+} counterions, present after primary calcination. This change is also supported by the UV/VIS spectra (see below). Formation of PtO clusters inside the zeolite cavities would explain the experimental results. Formation of PtO was suggested by Chmelka *et al*. (8) in NaY zeolite; however, contrary to our assumptions, this was directly after the calcination of Pt tetrammine ions. Formation of Pd^{2+} after calcination of Pd tetrammine in KL zeolite and PdO after recalcination was suggested in Ref. (10), and a decrease of the reduction temperature after recalcination of Pd was reported in Refs. (7, 10).

The complex character of the TPR curves does not allow us to draw conclusions on the effect of alkali ions. Hydrogen adsorption after the TPR can be related, according to Refs. (13, 14), to the average particle size of about 2 nm. The hydrogen consumption during the reduction roughly agrees with the reduction of all Pt, which was not observed with samples in which the Pt tetrammine ions were decomposed in vacuum (1, 2). The "incomplete" reduction in the latter case was explained by the participation of only surface layers of larger Pt clusters in redox cycles. The clusters formed via calcination of the tetrammine complex are therefore assumed to be small enough to expose the majority of Pt atoms to reduction and/or oxidation.

UV/VIS Measurements

As the shape of the TPR curves of calcined samples was assumed to reflect the presence of cationic Pt^{2+}, compensating the skeleton charge, it is tempting to assign the broad band at 550–630 nm to Pt^{2+} coordinated to three oxygens of the sodalite six-oxygen rings. The disappearance of this band in our spectra after cooling might be caused by adsorption of water vapor changing the coordination of Pt^{2+}. This band is not present after recalcination, when Pt is transformed to oxidic Pt species. Similarly, Homeyer and Sachtler (15) observed a band at 478.5 nm in calcined PdNaY samples and assigned it to "naked" Pd^{2+} ions. As regards the bands below 300 nm, it is difficult to ascribe them to individual species. The band near 250 nm, which was always found after reduction (Figs. 3B and 3D), may originate from plasma resonance of metallic particles (16–18). Studies on the interpretation of these bands are in progress.

Isotopic Exchange Reactions

Both the $H_2 + D_2$ and the $^{18}O_2 + {}^{16}O_2$ equilibrations as well as the ^{18}O heterophase exchange with the zeolite oxygens proceed very slowly over calcined samples, which means that Pt^{2+} ions compensating the skeleton charge are of low activity. The most rapid isotope exchange occurs over Pt^0. Recalcined Pt (Pt_{ox}, presumably PtO) also exhibits a considerable activity, in some cases (e.g., oxygen equilibration) indistinguishable from that of Pt^0.

Metallic platinum is commonly known to dissociate hydrogen very easily, so that the high activity in D_2–H_2 equilibration over reduced samples even at $-78^\circ C$ is not surprising. The relatively high activity of recalcined Pt (Pt_{ox}) might be due to a small amount of Pt^0 formed by reduction even at this temperature.

Regarding the oxygen exchange, the equilibration starting at about 300°C over metallic Pt points either to a relatively (compared to hydrogen) difficult dissociation of O_2 molecules or to recombination of dissociated oxygen atoms. This agrees with Refs. (19–21), where the recombination of oxygen atoms at about 400°C was reported.

The temperature at which the heterophase exchange (exchange between solid and gas phase (12)) can be reasonably measured is 380°C. At the same temperature the oxidation of Pt^0 in zeolitic cavities occurs (according to the repeatable TPR after reoxidation at 400°C), so that both Pt^0 and Pt_{ox} are probably present during the exchange, and therefore the exchange proceeds over recalcined samples with

almost the same rate as over those which were reduced. It is not possible from the kinetics of the isotopic exchange to separate the participation of the oxygen of Pt_{ox} from oxygens of the zeolite skeleton; however, the amount of oxygen which can be related to Pt is very small if compared with the number of oxygens in the zeolite framework.

It is known from the literature that oxygens of the zeolite skeleton are able to be exchanged for gaseous oxygen at relatively high temperature (above 600°C) and that the presence of cations decreases this temperature [e.g., Refs. (22–26)]. The relatively low temperature of the isotopic exchange of zeolitic oxygens with gaseous oxygens over Pt containing zeolites stresses the role of Pt in activating the oxygen molecules, and the ability of activated oxygens to be exchanged for the oxygens of the zeolite skeleton. The transfer of these activated oxygen species should proceed via spillover, as the Pt concentration in our sample is very low (about 3 Pt atoms per unit cell). The rapid (if compared with the heterophase oxygen exchange) equilibration of oxygen molecules proceeding simultaneously with the heterophase exchange did not allow us to determine the mechanism of the latter reaction (single or multiple).

CO + NO Reaction

Similarly to the above exchange reactions, the reduction of NO by CO proceeds most easily over metallic Pt which is known to catalyze NO decomposition [e.g., Ref. (28)]. Pt_{ox} in recalcined samples is easily reducible by CO, which can enhance the CO + NO reaction compared to Pt^{2+} in calcined samples (Fig. 7). The difference between the individual Pt states decreases with increasing temperature and virtually none is observed at 230°C.

It follows from all the catalytic tests employed that calcined platinum, most probably Pt^{2+}, exhibits the lowest activity. Once the charge-balancing effect is destroyed (Pt^0 and/or Pt_{ox}), platinum clusters become more active (metallic Pt ≥ Pt_{ox}). As mentioned above, slight reduction of Pt_{ox} during the hydrogen equilibration (−78°C) and in the NO reduction by CO cannot be excluded; however, in oxygen equilibration and heterophase oxygen exchange, which both proceed under oxygen atmosphere, the enhancement of activity by Pt_{ox} (compared to Pt^{2+}) clearly operates. This can be due to an easier weakening of the Pt–ox bond in the zeolite channels than that of $O^-_{zeol}Pt^{2+}O^-_{zeol}$ at ~400°C, which is the temperature of the heterophase oxygen exchange.

CONCLUSIONS

Calcination, Reduction, Recalcination—Pt State

(i) The calcination + reduction of Pt tetrammine ions in X and Y alkali zeolites leads to the formation of small Pt clusters, all of whose Pt atoms can be oxidized or reduced (contrary to larger clusters created during vacuum decomposition).

(ii) Calcination is assumed to yield predominantly Pt^{2+} ions which are less reducible than Pt_{ox} clusters formed via recalcination after the first reduction.

Catalytic Reactions over NaX and KX Zeolites with Pt of Different States

All the reactions studied were enhanced by different states of Pt in the sequence $Pt^0 > Pt_{ox} \gg Pt^{2+}$. Due to the treatment of the zeolite samples, formation of Pt^0 is accompanied by the formation of protons which compensate the zeolite skeleton charge instead of primarily Pt^{2+}. Protons also remain, at least partially, after recalcination, as Pt_{ox} clusters do not completely balance the zeolite charge.

$D_2 + H_2$ Equilibration

Hydrogen molecules are easily activated over Pt^0 clusters even at −78°C.

Oxygen Equilibration and Heterophase Exchange

The activation of oxygen molecules for the equilibration reaction over Pt proceeds above 300°C. The activated oxygen species are able to be exchanged for zeolitic oxygens (heterophase exchange) with a reasonable rate at about 400°C. The spillover of these species toward zeolitic oxygens should be assumed. The equilibration (homophase) reaction starts above 300°C and proceeds then very quickly. The heterophase exchange includes transfer of the activated oxygen species (which can be equilibrated without the incorporation of the zeolite oxygen and therefore more rapidly) to the oxygens of the zeolitic skeleton, which weakening necessary for the exchange needs a higher temperature.

ACKNOWLEDGMENTS

This work was supported by Grants GA AVCR(440105) and GA CR (203/96/0951). The authors thank Professor G. Schulz-Ekloff and the referees for valuable discussions and Dr. P. Hülstede for measurement of the UV/VIS spectra.

REFERENCES

1. Nováková, J., Brabec, L., and Kubelková, L., *Collect. Czech. Chem. Commun.* **60**, 428 (1995).
2. Nováková, J., Kubelková, L., Brabec, L., Schulz-Ekloff, G., and Jaeger, N., *Zeolites* **16**, 173 (1996).
3. Exner, D., Jaeger, N., and Schulz-Ekloff, G., *Chem. Ing. Tech.* **52**, 734 (1980).
4. Jaeger, N., Jourdan, A. L., and Schulz-Ekloff, G., *J. Chem. Soc. Faraday Trans.* **87**, 1251 (1991).
5. Schulz-Ekloff, D., and Jaeger, N., *Catal. Today* **3**, 459 (1988).
6. Gallezot, P., *Catal. Rev. Sci. Eng.* **20**, 122 (1979).
7. Sachtler, W. M. H., and Zhang, Z., *Adv. Catal.* **39**, 129 (1993).
8. Chmelka, B. F., Went, G. T., Csencsits, R., Bell, A. T., Petersen, E. E., and Radke, C. J., *J. Catal.* **144**, 506 (1993).

9. Ryoo, R., Cho, S. J., and Pak, Ch., *Catal. Lett.* **20**, 107 (1993).
10. Ostgard, D. J., Kustov, L., Poeppelmeier, K. R., and Sachtler, W. M. H., *J. Catal.* **133**, 342 (1992).
11. Bastl, Z., Kubelková, L., and Nováková, J., *Zeolites*, submitted.
12. Nováková, J., *Catal. Rev.* **4**, 77 (1971).
13. Bond, G. C., *Chem. Soc. Rev.* **20**, 441 (1991).
14. Ponec, V., and Bond, G. C., *in* "Catalysis by Metals and Alloys. Vol. 95. Studies in Surfinactent Science and Catalysis," p. 228. Elsevier, 1995.
15. Zhang, Z., and Sachtler, W. M. H., *Zeolites* **10**, 784 (1990).
16. Kubelková, L., Vylita, J., Brabec, L., Drozdová, L., Bolom, T., Nováková, J., Schulz-Ekloff, G., and Jaeger, N. I., *J. Chem. Soc. Faraday Trans.* **92**, 2035 (1996).
17. Crighton, J. A., and Eldon, D. G., *J. Chem. Soc. Faraday Trans.* **87**, 3881 (1991).
18. Benfield, D. E., Maydwell, A. P., van Ruitensbeck, J. M., and van Leeuwen, D. A., *Z. Phys.* **26** (Suppl.), 4 (1993).
19. Gland, J. I., *Surf. Sci.* **93**, 487 (1980).
20. Akhter, S., and White, J. M., *Surf. Sci.* **171**, 527 (1986).
21. Sawabe, K., Matsumoto, Y., Yoshinolu, J., and Kawai, M., *J. Chem. Phys.* **103**, 4757 (1995).
22. Minachev, Kh. M., Savostjanov, E. N., Kondrateev, D. A., Tchan Zui Nuui, and Antoshin, G. V., *Izv. Akad. Sci. USSR Ser. Khim.*, 841 (1971).
23. Fu, C. M., Korchak, V. N., and Hall, W. K., *J. Catal.* **68**, 166 (1981).
24. Leglise, J., Petunchi, J. O., and Hall, W. K., *J. Catal.* **86**, 392 (1984).
25. Tkatchenko, O. P., Antoshin, G. V., Minachev, Kh. M., Portchidze, G. V., Tsitsisvili, G. V., and Tsintsikaladze, Z. P., *Izv. Akad. Sci. USSR Ser. Khim.*, 1716 and 1718 (1986).
26. Chang, Y. F., Somorjai, G. A., and Heinemann, H., *J. Catal.* **154**, 24 (1995).
27. Altman, E. I., and Gorte, R. J., *J. Phys. Chem.* **93**, 1993 (1989).
28. Brabec, L., to be submitted.